Fractionation of aqueous isopropanol mixtures in a countercurrent packed column using supercritical CO2

R. Lalam, Saousan Chamali, Séverine Camy, David Rouzineau, R. Kessas, Jean-Stéphane Condoret

To cite this version:

Fractionation of aqueous isopropanol mixtures in a countercurrent packed column using supercritical CO_2

R. Lalam [a], S. Chamali [b], S. Camy [b,*], D. Rouzineau [b], R. Kessas [a], J.-S. Condoret [b]

[a] Université des Sciences et de la Technologie d'Oran – Mohamed Boudiaf, BP 1505 El-M'Naouar, Oran, Algeria
[b] Université de Toulouse, INPT, UPS, Laboratoire de Génie Chimique UMR CNRS 5503, 4, Allée Emile Monso, F-31030 Toulouse, France

ARTICLE INFO

ABSTRACT

Purification of isopropanol aqueous mixtures by supercritical CO_2 was realized in the continuous mode using a packed column. The aim of the study was to experimentally and theoretically evaluate the separation performance of this packed contactor. Experiments were performed in a column of 2 m height and 17 mm diameter, in the range (10–20 MPa) and (40–60 °C) with a solvent to feed ratio varying from 4 to 11. Two types of packing, spring shape packing and metallic foam, were tested. The IPA composition of the feed was varied between 5% and 60% (w/w). The experimental results were compared to simulation of the process using the process simulation software Prosim Plus. The column modelling was based on the concept of theoretical equilibrium stages. Thermodynamic behaviour of the CO_2–IPA–water system under pressure was represented on the whole range of conditions corresponding to the process, using the Soave–Redlich–Kwong equation of state (SRK) modified by Boston Mathias with PSRK mixing rules and UNIQUAC activity coefficient models. This model gave the best predictions, after the twelve interaction coefficients (four for each binary subsystem) were identified from the literature equilibrium experimental data. From the modelling, rather high values of the Height of a Theoretical Stage (HETS) were obtained (larger than 1 m) and these values were shown to diminish when the IPA feed composition was increased.

1. Introduction

Isopropanol (IPA) is a secondary alcohol currently used as a chemical feedstock in particular for acetone production and also as a solvent in many consumer products [1]. Although IPA is currently obtained via indirect or direct hydration of propylene, some alternative bio-processes are under investigations. These alternatives routes have to meet the recent green chemistry requirements which encourage the use of bio sourced chemicals. Fermentation routes for IPA have been investigated with several species of *Clostridium* leading to so-called bio-isopropanol. Nevertheless, IPA concentrations obtained with these strains were very low because clostridia produce butanol together with IPA [2], although Inokuma et al. [3] have recently shown that fermentation of glucose using metabolically engineered *Escherichia coli* strain TA76, could lead to IPA aqueous solution. Nevertheless, recovery of IPA from fermentation broth is usually proposed by distillation of the azeotropic isopropanol/water mixture. This route implies a high energy consumption and alternative downstream processes for purification of these bio alcohols need to be proposed.

Use of supercritical fluids for fractionation of ethanol–water mixtures has been studied for long, considering the interest to propose alternative processes to the azeotropic distillation for this mixture. This was envisaged for applications such as dealcoholisation of beverages [4], extraction of aromatic compounds from alcoholic solutions [5] or purification of bioethanol [6]. This kind of separation can be operated in continuous mode, in spray, packed or sieve-tray columns, where liquid phase to be fractionated flows counter-currently with the supercritical solvent, in a similar way as liquid–liquid extraction. Also, supercritical fractionation has been proposed, at laboratory or pilot scales, for deacidification of edible oils [7], fish oils fractionation [8], deterpenation of citrus oils [9], or fractionation of perfluorinated oligomers [10]. Although still underexploited, the potential of this technology for industrial applications is thus significant, but a better understanding of the process is still needed for its full development, as recently stated by Brunner [11].

Specific studies above mass transfer performances in countercurrent fractionation columns, for processing aqueous solutions of alcohols with supercritical carbon dioxide or other solvents, are available in the literature. For instance, Rathkamp et al. [12]

and Lahiere and Fair [13] studied separation of ethanol/water and isopropanol/water with supercritical CO_2 in spray, sieve tray and Rashig ring packed columns (1.2 m height and 2.54 cm internal diameter). Values of global mass transfer parameters such as Height and Number of Transfer Unit (HTU/NTU) and Height Equivalent to a Theoretical Stage (HETS) have been deduced from experimental results and compared to conventional liquid–liquid systems. The authors pointed out that, despite high mass transfer coefficients in the supercritical phase, important resistance to mass transfer occurred in that phase due to low partition coefficients of alcohols. Several mass transfer studies have been done about the CO_2/water/ethanol system such as the one of Bernad et al. [14] using a countercurrent 1.4 m height and 54 mm internal diameter column, packed with stainless steel BX 64 Sulzer packing. Commercial, so as home-made simulation softwares were used by the authors to estimate HETS of the contactor and comparison of two contacting modes (trickle bed and bubble column) was done. HETS values were found to range between 0.5 and 1.5 m depending on experimental conditions and contacting mode, the packed bubble column being the most efficient. Also, Lim et al. [15], using a 3.175 cm internal diameter and 1.52 m height Knit mesh elements packed column, extensively studied this system and showed that conventional mass transfer models used for liquid–liquid extraction could be used with a reasonable accuracy to predict overall mass transfer coefficient. Using the graphical Ponchon–Savarit method, Budich and Brunner [16] showed that it was theoretically possible to obtain anhydrous ethanol when operating extraction at 333 K and 10 MPa, where the ternary system exhibits so-called type II thermodynamic behaviour (taking advantage of the ethanol–CO_2 partial immiscibility). The CO_2–1-butanol–water system was studied by Laitinen and Kaunisto [17] who showed the feasibility of the separation using $scCO_2$ at 10 MPa and 313 K in a mechanically agitated Oldshue-Rushton-type column (2 m high and 35 mm internal diameter). From the HTU–NTU approach, they deduced values of overall mass transfer coefficients of the system and HETS were found to be in the range 0.4–0.5 m. Moreover, they evidenced that mechanical agitation had no effect on the column efficiency at the selected extraction conditions.

A better understanding of mass transfer should arise from the knowledge of hydrodynamics of high pressure countercurrent contactors but such studies are very scarce, mainly due to experimental difficulties for measuring pressure drops or visualizing flow patterns in high pressure systems. Most studies have concerned measurements of liquid hold-up in the column using static methods [15] and analysis of flooding of the column was done with a column equipped with sapphire windows and pressure drop transducers [16]. These studies essentially highlighted that hold-up is greater in packed columns as compared to spray columns. Also, flooding conditions were shown to be influenced by the ethanol content in the feed, because of its influence on fluid properties.

Most engineering studies have utilized conventional chemical engineering tools, similar to those for liquid–liquid extraction, but, when thermodynamic behaviour of the mixture can be satisfactorily described using standard thermodynamic models, such as cubic equations of state, commercial process simulation softwares are useful tools to model a fractionation column and/or the entire process, including solute recovery and solvent recycling. Bernad et al. [14] used the ProSim software to estimate HETS values of their experimental set-up in the case of ethanol recovery from aqueous solutions. The ASPEN Plus software was successfully used by Brunner [18] and Riha and Brunner [19] to evaluate the number of theoretical stages of their experimental set-up and to predict the concentration profiles in a column used to process a mixture of ethyl esters of fatty acids. They showed that Aspen Plus led to similar HETS values than those obtained from conventional graphical Mc Cabe and Thiele or Ponchon–Savarit methods. Recently, Fiori

et al. [20] used the same software to investigate and optimize the fractionation of omega-3 lipids from fish oil by supercritical CO_2. Similarly, the HYSIS software was used by Moraes et al. [21] in order to optimize a process for dehydration of ethanol using supercritical propane. Typically, with these approaches, counter-current contactors are represented by a succession of equilibrium theoretical stages. With a proper thermodynamic model, these tools provide information on separation performances, together with other information such as energy consumption of the process or optimized experimental conditions for solute recovery. Considering the ongoing improvements of these tools, with implementation of novel thermodynamic models, use of simulation softwares in the design and optimization of operating conditions of such processes appear now as unavoidable.

Indeed, the objective of our work was to consider the CO_2 fractionation of aqueous IPA mixtures to give an analysis of experimental separation results using a process simulation software (here the ProSim Plus software), fed with the adapted thermodynamic model. For that purpose, specific effort was done to model the ternary fluid phase equilibrium of the CO_2–water–IPA system. Use of an adapted thermodynamic model is indeed expected to improve description of the column operation since, in previous works about fractionation of aqueous isopropanol mixtures [12,13] the thermodynamics behaviour of the system was represented by a simplified approach based on the use of a constant partition coefficient.

2. Materials and methods

2.1. Materials

Carbon dioxide was supplied by Air Liquide (≥purity 99.98%) and isopropanol is from Sigma–Aldrich (≥purity 99.8%). Distilled water was used for aqueous mixtures preparation.

2.2. Experimental set-up

The experimental set up (Fig. 1) was purchased from the Separex Company (Champigneulles, France). This device consists of a 2 m high column with 17 mm internal diameter, filled with random packing made of "spring" shaped stainless steel elements (see photo in Table 1) whose dimensions are 5 mm length and 3 mm diameter. The wire diameter of the spring is 0.55 mm and its extended length is 62 mm. The specific surface of this packing was theoretically evaluated from the number of elements per unit volume (experimentally determined by manual counting) and computation of the surface of an element. If it is assumed to evaluate the specific surface considering the entire surface of the wire constituting the spring, the value of the specific surface of the packing is then computed at $a = 1184 \, m^2/m^3$. The void fraction ε was experimentally measured at 0.75. This measurement was done in a tube of the same diameter as the column, thus including wall effects.

In this work an original packing made of open cellular metallic (FeCrAlY) foam (5 Pores per Inches, characteristic dimension of pores 4 mm) was also tested. It is composed of 5 cm high, 17 mm diameter cylindrical pieces that were cut out from blocs of metallic foam (using water jet technology) and stacked inside the column. Its void fraction is 0.92 and its specific surface is equal to $a = 610 \, m^2/m^3$, evaluated elsewhere [37]. Characteristics of both packings are gathered in Table 1.

The column is equipped with four type J temperature sensors (±1 °C) distributed along the column wall and temperature is regulated by an electrical heating device. Pressure is measured by a 0–400 bar manometer (±2 bar). A specific device made of two automatic valves in series, alternatively closed and opened by a
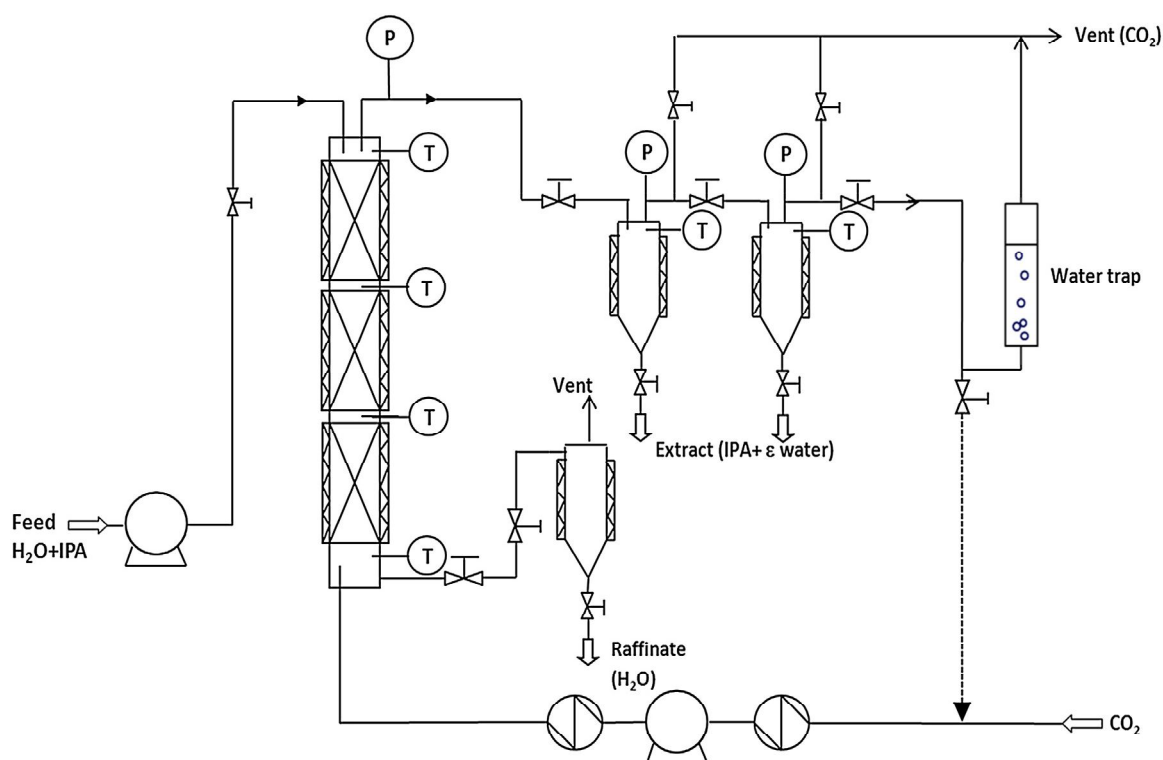
Fig. 1. Experimental set-up.

timer, placed at the bottom of the column, is used to recover the raffinate in a pseudo-continuous mode. For each liquid flowrate, frequency and duration of opening and closure of the valves are beforehand determined, in order to ensure a constant level of liquid at the bottom of the column. For instance, for a liquid flowrate equal to 0.48 kg/h the opening duration of the second valve and closing duration of the first one is 1 s, every 9 s.

At the top of the column, two separators in series allow recovering the liquid extract, free of CO_2. Imperfect separation of the extract in the separators was observed. Therefore a water trap (*i.e.*, micro-bubbling of the effluent gas in a vessel filled with water), was placed at the output of the second separator to limit losses of IPA due to mechanical entrainment in the separators as frequently observed in small size separators. Indeed, cyclonic separators used in this study were initially designed to recover heavy compounds such as lipid fractions extracted from plant material by supercritical CO_2. In a previous study we evidenced existence of important mechanical entrainment when these devices are used to recover

volatile compounds such as alcohols, for example in the context of co-solvent recovery [22]. However, in spite of an improvement observed with the water trap, mass balances on the column evidenced that the set-up for extract recovery was still imperfect and a non-negligible part of solute was lost. Consequently, in this study, analysis of column performances was only based on measurement of flowrates and composition of the raffinate (bottom) phase. Values of composition and flowrate of extracts were thus obtained from a mass balance computation over the column. Note that this problem has already been reported by authors processing volatile alcohol such as ethanol [12,13]. Moreover, although the pilot could be operated with a CO_2 recycle loop, it was operated in open loop for easier interpretation of results.

The extraction procedure was as follows: the output liquid from the CO_2 bottle (about 5.5 MPa) is subcooled in a heat exchanger up to 5 °C and then pumped using a high pressure positive displacement diaphragm pump (Milton Roy Dosapro®) with a maximum capacity of 5 kg/h. The CO_2 flowrate is measured with Coriolis type

Table 1
Packings characteristics.

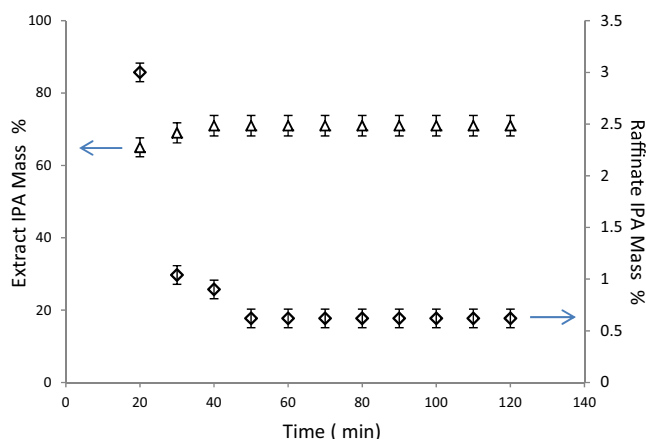| Type	Springs	Foam
Dimensions	5 mm length 3 mm diameter	5 cm high and 17 mm diameter cylinders with 4 mm pores
Material	Stainless steel	FeCrAlY
Specific surface (m²/m³)	1184	610
Void fraction	0.75	0.92

Fig. 2. Time course of experimental raffinate ($\Diamond$) and extract (Δ) composition for fractionation at 10 MPa, 40 °C, $S/F = 9.5$, feed containing 5% (w/w) of IPA.

flowmeter (Micro Motion, D6 model, known at ± 0.5 g/min). The pressurized liquid CO_2 is then heated to the desired temperature for the extraction. The CO_2 is fed at the bottom of the column and flows countercurrently with the liquid water–IPA mixture feed which is pre-heated to 40 °C and introduced at the top of the column using a high pressure membrane pump (Milton Roy Dosapro®) with a maximum capacity of 2.4 kg/h. The pump feed flowrate was calibrated using a gravimetric method (± 0.17 g/min). The column is operated in the trickle bed mode, supercritical CO_2 being the continuous phase. Operating conditions at the raffinate separator were 20 °C and atmospheric pressure. The CO_2 rich mixture (extract) at the top of the column flows through a set of two cyclone separators ($V = 40$ mL) in series. Pressure in the column is regulated by a back pressure regulator (TESCOM 44-23 Series). The extract was recovered at 6 MPa and 23 °C in the first separator, 0.1 MPa and 0 °C in the second one and room temperature in the water trap. Analyses of the compositions of the different liquid phases were performed by refractometry technique.

Note that because our results are only based on raffinate measurements and mass balance, it is crucial to ascertain steady state and reproducibility. Around 40 min were usually needed to obtain steady-state operation whose obtaining is assumed when raffinate and extract composition are constant over around 1 h, as shown in Fig. 2 for a typical experiment (40 °C, 10 MPa, $S/F = 9.5$ and IPA feed mass fraction 5%). Each run was reproduced in quadruplicate and results were found reproducible (the mean deviation was 0.005% for raffinate IPA mass fraction and 0.35% for raffinate IPA recovery ratio). Assessment of reproducibility of experiments is illustrated in

Fig. 3, where raffinate IPA recovery ratio (a) and raffinate IPA mass percent (b) are indicated in the case of four experiments realized at 10 MPa and 40 °C. In this study, raffinate recovery ratio is obtained by dividing raffinate IPA flow rate by feed IPA flowrate.

Experimental fractionation of diluted aqueous solutions of IPA (5%, w/w) were first experimentally studied using the stainless steel spring packing and influence of pressure, temperature and solvent to feed ratio was evaluated. Fractionation of more concentrated feed solutions was also investigated. Finally, impact of the packing type was studied, comparing with results obtained with the metallic foam packing.

3. Thermodynamic modelling of the ternary mixture

Knowledge of phase equilibria of the ternary mixture is essential to understand and analyze the process of fractionation. Furthermore, in view of process simulation, a model capable of representing the phase equilibria must be selected among available models and validated by comparison with equilibrium experimental data. Experimental data for this mixture exist in the literature, for pressures ranging from 6.89 to 30 MPa and temperatures between 15 and 70 °C [23,24]. In this study, these data were modelled using the Simulis® Thermodynamics software (ProSim SA) in the Excel environment (Microsoft). Given the pressure range and the highly polar nature of water and isopropanol, the combined approach equation of state/activity coefficient (EoS/G^E) model, using a suitable complex mixing rule, was chosen. In this approach, the behaviour of the fluid mixture is represented by an equation of state over the entire fluid range. The combined approach allows extending the field of application of original equations of state (high pressure with low polarity compounds) to mixtures containing polar compounds, by incorporating the excess Gibbs energy G^E in the calculation of the energy term a of the equation of state. The excess Gibbs energy is calculated using an activity coefficient model. Huron and Vidal [25] were the first to propose this approach, and several models based on this concept were then developed, such as Wong-Sandler, MHV1, MHV2 or PSRK, and were successfully applied to describe high pressure phase equilibria for mixtures containing polar compounds with compounds such as CO_2. The equation of state chosen in this study is the well-known Soave–Redlich–Kwong equation [26] with the modification proposed by Boston-Mathias [27], which is suitable for mixtures containing compounds above their critical temperature. The co-volume term of the SRK equation is obtained from a standard mixing rule (arithmetic mean of the parameters of the pure substances). The mixing rule PSRK [28] was chosen here to compute the energy term of the SRK equation of state. Several activity coefficient
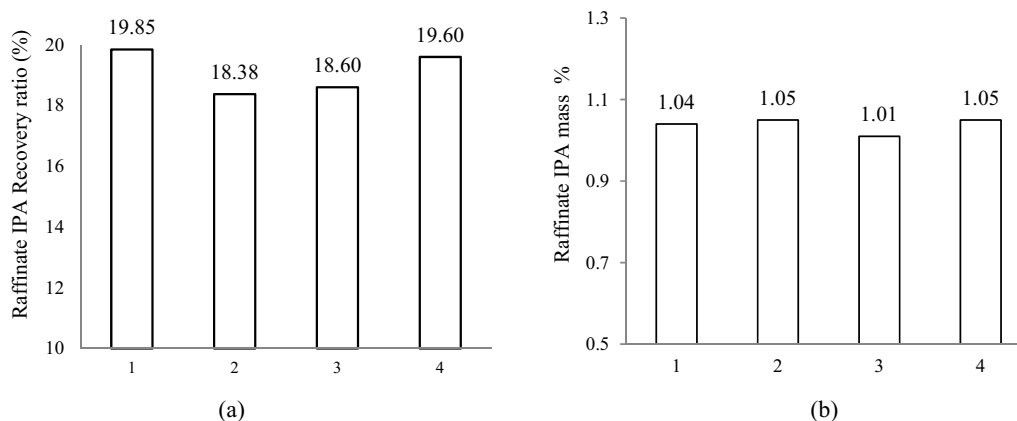

Fig. 3. Reproducibility of fractionation at 10 MPa, 40 °C, $S/F = 6$ and feed containing 5% (w/w) of IPA. Experiment realized in quadruplicate.

Table 2
SRK-PSRK-UNIQUAC model fitting results from the literature binary experimental data.

i	j	Data type Ref.	Range	Np	A_{ij}	A_{ji}	$AAREx_i$ (%)	$AAREx_j$ (%)	$AAREy_i$ (%)	$AAREy_j$ (%)
CO_2	IPA	P-x,y [31]	[316.5 – 394] K [5.86–12.41] MPa	21	$402.63 - 0.0355\,T$	$213.52 - 0.975\,T$	6.57	5.64	0.6	8.29
CO_2	H_2O	P-x [32]	[308–348] K [0.101–3.647] MPa	57	$19.99 + 2.416\,T$	$-426.05 + 3.783\,T$	3.91	0.02	–	–
		P-y [33]	[298–373] K [2.26–5.14] MPa	21			–	–	0.07	9.87
IPA	H_2O	P-x,y [34]	[423–473] K [0.517–2.613] MPa	37	$95.628 + 0.293\,T$	$97.14 + 0.441\,T$	26.51	4.08	4.02	3.02

models such as UNIQUAC or UNIFAC (predictive model) were tested to calculate the excess energy at zero pressure G^{E0}, involved in PSRK mixing rule for the ternary CO_2–IPA–water mixture.

The best predictions were obtained by using UNIQUAC [29,30] model, with temperature dependent binary interaction parameters. For the ternary system, twelve coefficients (four for each binary subsystem) have to be fitted, which makes the experimental data fitting procedure highly dependent of initialization values. To overcome this problem, literature liquid–vapour equilibria data for binary subsystems were used to find a set of binary interaction parameters which were then used as initialization values in the procedure for fitting of data of the ternary mixture. The objective function to be minimized in the fitting procedure was:

$$Fobj = \frac{1}{N_p} \sum_{j=1}^{Np} \left(\sum_{i=1}^{Nc} \left| \frac{y_i^{exp} - y_i^{calc}}{\left(\frac{y_i^{exp} + y_i^{calc}}{2} \right)} \right| + \sum_{i=1}^{Nc} \left| \frac{x_i^{exp} - x_i^{calc}}{\left(\frac{x_i^{exp} + x_i^{calc}}{2} \right)} \right| \right) \quad (1)$$

where x_i and y_i are liquid and vapour mole fraction of compound i, respectively, Np is the total number of points and Nc the number of compounds. Values of binary interaction parameters (BIP) obtained from binary vapour–liquid equilibrium data and subsequent mean Average Absolute Relative Error (*AARE*) defined for any molar fraction z_i in Eq. (2), are indicated in Table 2.

$$AAREz_i = \frac{100}{N_p} \sum_{i=1}^{Np} \left| \frac{z_i^{exp} - z_i^{calc}}{z_i^{exp}} \right| \quad (2)$$

As mentioned above, values of BIPs presented in Table 2 have then be used as initialization values to determine a set of BIPs allowing a better fitting of CO_2–IPA–water ternary equilibrium data from [23,24] by minimizing the objective function presented in Eq. (1). Corresponding results are gathered in Table 3. *AARE* of liquid and vapour mole fractions have been calculated from 43 points of [23] to 16 points of [24].

An example of comparison of experimental data and values calculated by the SRK-PSRK-UNIQUAC model with BIPs presented in Table 3 is shown in Fig. 4. As it can be observed, the model provides a good qualitative and quantitative representation of the experimental behaviour of the ternary system. So,

simulations of fractionation process were performed with the SRK-PSRK-UNIQUAC model using this set of BIPs.

As reported in Tables 4 and 5, most fractionation experiments were conducted at 40 °C and 10 MPa. Under these conditions, the thermodynamic behaviour of the ternary system, calculated with the SRK-PSRK-UNIQUAC model, is represented in mass fractions in Fig. 5(a). At 40 °C and 10 MPa, the behaviour appears to be of the so-called type I (in reference to the conventional classification of ternary mixtures of liquid–liquid systems). For type I behaviour, partial immiscibility only exists between water and CO_2 and not between CO_2 and isopropanol. In this configuration, conventional analysis for liquid–liquid extraction states that anhydrous isopropanol cannot be recovered at the top of the column. The theoretical reachable maximum purity for isopropanol is then around 97% (w/w), obtained by the intercept of the tangent to the equilibrium curve with the opposite side of the triangle, as shown in Fig. 5(a). Nevertheless, it is possible to obtain conditions where CO_2–IPA partial immiscibility exists. For example, at 10 MPa and 61.8 °C, it can be seen that, whatever the composition, the binary mixture is single phase whereas a two-phase zone appears at higher temperature or at lower pressure. In this case, the ternary system consequently switches to type II behaviour, as shown for example at 70 °C and 10 MPa in Fig. 5(b). Maximum theoretical purity of IPA in that case can reach 100%. Budich and Brunner [16] have shown that for fractionation of ethanol aqueous solution, type II behaviour allowed obtaining ethanol above its azeotropic concentration. However, because of poorer solubility of ethanol in CO_2 compared to IPA, conditions of partial immiscibility of CO_2 and ethanol occur in a larger range than for the CO_2–IPA system.

Variation of the distribution coefficient of IPA in respect to the liquid phase IPA mass fraction has been computed using the model and is shown in Fig. 6. For low IPA liquid mass fraction, a moderate increase of the IPA distribution coefficients with liquid IPA mass fraction can be observed, especially at high temperature. So, better accuracy of the modelling can be expected with our thermodynamic model, in comparison with modelling using constant distribution coefficient, as was often done in previous works. Also, at 10 MPa, increasing temperature in the range 40–60 °C is observed to reduce the IPA distribution coefficient, while at 20 MPa, this coefficient is only slightly influenced by temperature.

Table 3
SRK-PSRK-UNIQUAC model fitting results of ternary experimental data from [23,24].

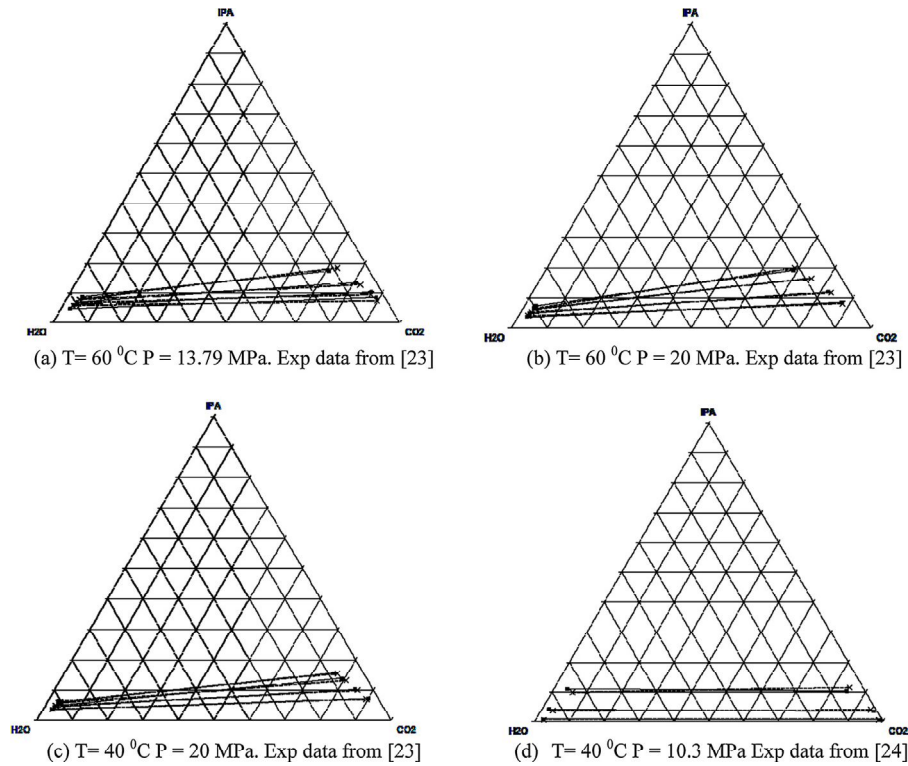| i	j	A_{ij}	A_{ji}	$AAREx_{CO2}$ (%)	$AAREx_{IPA}$ (%)	$AAREx_{H2O}$ (%)	$AAREy_{CO2}$ (%)	$AARy_{IPA}$ (%)	$AARy_{H2O}$ (%)
CO_2	IPA	$408.19 - 0.54\,T$	$379.7 - 1.16\,T$						
CO_2	H_2O	$-49.65 + 3.098\,T$	$-509.20 + 4.80\,T$	22.08	9.33	2.11	2.75	13.35	26.23
IPA	H_2O	$-135.53 + 0.437\,T$	$223.98 + 0.376\,T$						

Fig. 4. Phase diagrams of the ternary CO_2–IPA–water system (mole fractions). Comparison of experimental data from [23,24] (solid lines) and calculated tie-lines (dashed lines) with SRK-PSRK-UNIQUAC model.

Table 4
Experimental runs for spring packing.

Run	Operating conditions				Raffinate (experimental results)			Extract (calculated by mass balance)	
	P (MPa)	T (°C)	S/F	Feed IPA (w%)	IPA (w%)	IPA recovery ratio (%)	Water recovery ratio (%)	IPA recovery ratio (%)	IPA (w%)
1	10	40	9.50	5	0.62	11.39	96.11	88.61	54.53
2	10	40	9.50	15	1.04	5.92	99.45	94.08	96.77
3	10	40	9.50	30	0.81	1.81	94.46	98.19	88.37
4	10	40	9.50	40	0.62	0.81	86.26	99.19	82.80
5	10	40	9.50	60	0.62	0.31	75.05	99.69	89.70
6	10	50	9.50	5	1.28	24.94	97.40	75.06	60.05
7	10	60	9.50	5	1.50	30.00	98.09	67.96	65.24
8	10	40	3.95	5	2.08	39.00	96.63	61.00	48.80
9	10	40	6.27	5	0.90	14.67	95.72	85.33	51.20
10	10	40	11.04	5	0.42	7.49	93.47	92.51	42.70
11	10	40	6.04	5	1.10	20.00	97.60	80.00	64.00
12	12	40	6.04	5	0.70	12.67	95.82	87.33	52.40
13	15	40	6.04	5	0.55	9.72	93.78	90.28	43.33
14	20	40	6.04	5	0.42	7.42	93.90	92.58	44.44

Table 5
Experimental runs for metallic foam packing.

| Run	Operating conditions				Raffinate (experimental results)			Extract (calculated by mass balance)	
	P (MPa)	T (°C)	S/F	Feed IPA (w%)	IPA (w%)	IPA recovery ratio (%)	Water recovery ratio (%)	IPA recovery ratio (%)	IPA (w%)
15	10	40	4.5	5	2.08	39.92	51.54	60.08	73.15
16	10	40	5.3	5	1.37	25.83	51.91	74.17	63.71
17	10	40	6.26	5	0.64	11.63	52.29	88.37	66.28
18	10	40	7.46	5	0.42	7.67	52.41	92.33	54.72
19	10	40	9.36	5	0.21	3.77	52.52	96.23	50.63
20	10	40	11.00	5	0.10	1.92	52.58	98.09	61.11
21	10	40	9.50	5	0.31	5.81	43.11	94.19	68.20
22	10	50	9.50	5	0.42	7.98	41.49	92.02	55.00
23	10	60	9.50	5	0.42	7.54	41.49	92.46	49.31
24	10	40	6.04	5	0.62	11.63	98.07	88.37	70.00
25	12	40	6.04	5	0.52	9.53	96.36	90.47	56.90
26	15	40	6.04	5	0.42	7.40	93.25	92.60	36.01
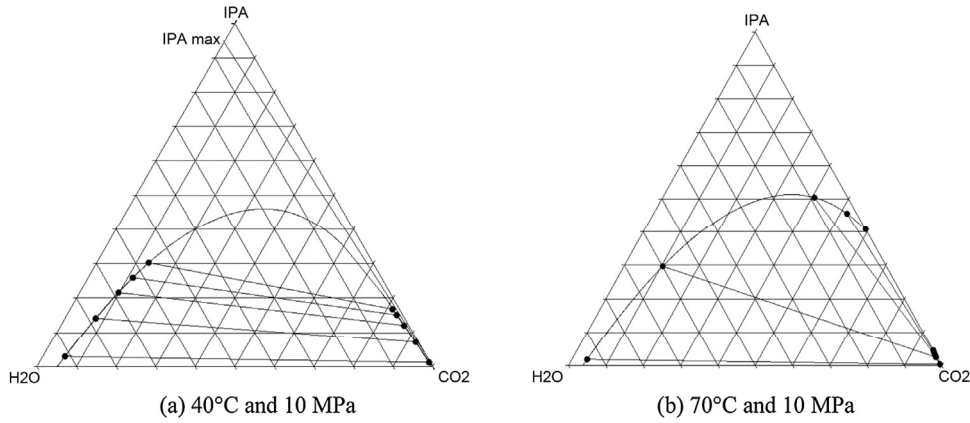
Fig. 5. Calculated fluid phase equilibrium of ternary CO_2–IPA–water system at 40 °C (a) and 70 °C (b) and 10 MPa (mass fractions).

4. Results and discussion

Experimental operating conditions and results, expressed in terms of isopropanol recovery ratio and isopropanol mass percent in the raffinate are gathered in Tables 4 and 5 for both packings. Corresponding extract isopropanol recovery ratio and purity (mass percent) obtained by mass balance from raffinate experimental results are given.

The ProSim Plus (Prosim S.A., France) software for simulation and optimization of steady-state processes was used to evaluate global performances of the separation column. The theoretical stages approach was used to simulate the column. Using this approach to model packed contactors is quite disputable, since this approach is actually issued from the description of multi-staged contactors with specific discrete structure, like tray columns for example, where the concept of thermodynamic equilibrium on a stage has a real physical meaning. For packed columns, the composition of phases is gradually changing along the column and the concepts of Number and Height of Transfer Unit, based on the representation of mass transfer fluxes between phases, have been developed to give a better description of this operation. However, convenient use of this approach would need to consider some simplifications (constant properties of fluids along the column height for example), finally also leading to disputable results. From the height of the column packing, the theoretical stages approach allows representing performances of the column thanks to the widespread concept of Height Equivalent to a Theoretical Stage (HETS), corresponding to the total height of the packed contactor divided by the Number of Equivalent Theoretical Stages (NETS),

this latter being obtained from experimental fractionation results. Although this value is actually dependent on operating conditions, nature and concentration of the system and type of packing, and so is intrinsically not generalizable, this approach has been and is still widely used to qualify packed contactors. For this reason, as a first approach, the NETS-HETS concept was used in this study to analyze separation performances of the experimental column.

4.1. Influence of pressure

Fig. 7 represents the influence of the pressure in the range 10–20 MPa, in the case of fractionation of a 5% (w/w) IPA aqueous solution at 40 °C, at 0.48 kg/h liquid feed flowrate with a solvent to feed ratio (S/F) equal to 6, using the column equipped with stainless steel spring packing. IPA mass fraction in the raffinate (on a CO_2 free basis) and IPA and water recovery ratios in the raffinate are plotted in Fig. 7(a) and (b), respectively.

A decrease of raffinate recovery ratios of both compounds (Fig. 7(b)) was observed when pressure was increased. This is explained by the increase of the CO_2 solvent power in respect to both compounds. This leads to lower IPA mass fraction in the raffinate (Fig. 7(a)) and therefore to an improvement of the purity of water at the bottom of the column. At 20 MPa (which actually corresponds to the maximum pressure of the experiments) the purity of water in the raffinate reached 99.6% with recovery ratios equal to 7.4% for IPA and 93.9% for water (Run 14). From mass balance, this corresponds to 92.6% IPA recovery in the top of the column and demonstrates the ability of our system to efficiently extract IPA. However, mass balance on IPA also indicates a 44.4% (w/w) IPA purity in the extract, which is a low value, indicating non-negligible co-extraction of water. Consequently, increasing pressure lowers the selectivity of CO_2 in respect to IPA and is not advisable in our case. This loss of performance can be explained from the evolution of the selectivity in respect to pressure. As an example, influence of pressure on selectivity α (defined as the ratio $(y_{IPA}/y_{water})/(x_{IPA}/x_{water})$) for a ternary system of given global composition at 40 °C is represented in Fig. 8. This curve has been obtained by plotting influence of pressure on calculated composition of vapour and liquid phases at equilibrium (one equilibrium stage) for a global composition of mixture z_i representative of a mixture entering the column ($F = 0.48$ kg/h with 5% (w/w) IPA and $S/F = 6$). Under these conditions, a maximum value of selectivity is observed at around 13 MPa.

Simulations of experimental runs were performed to evaluate the number of theoretical stages by fitting experimental values of IPA mass fraction and recovery ratios in the raffinate. On that base, it was found that modelling of the column with one theoretical stage only, actually led to under-estimation of extraction ratio of
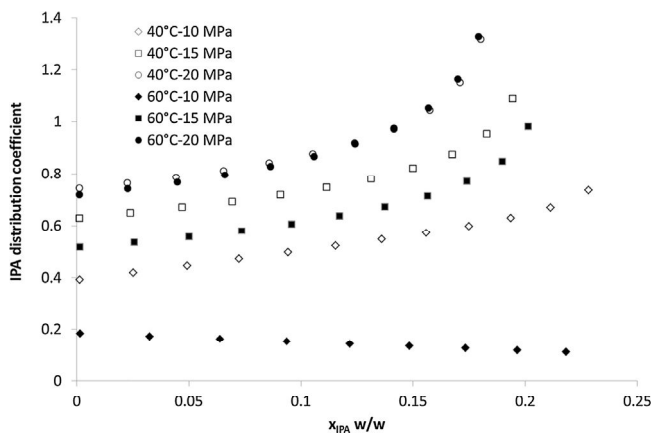

Fig. 6. Calculated IPA distribution coefficient (based on mass fractions of IPA) versus IPA mass fraction in liquid phase. Influence of pressure and temperature.
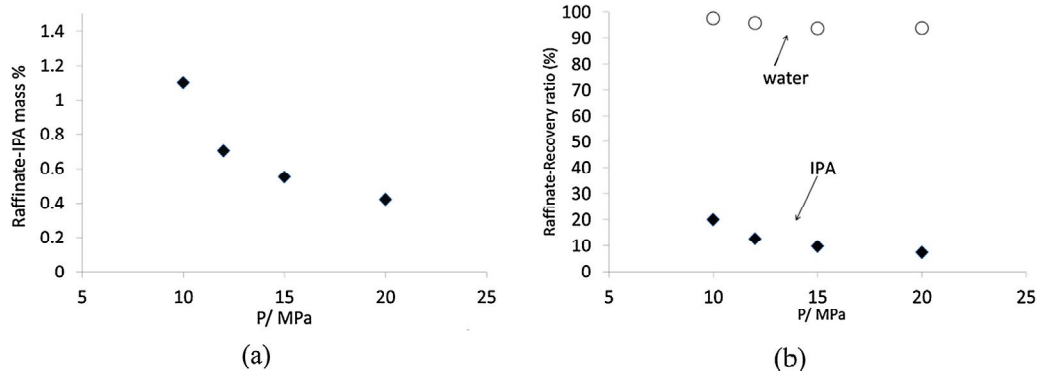
Fig. 7. Influence of the pressure on (a) IPA mass fraction in the raffinate and (b) IPA and water recovery ratio in the raffinate (40 °C, feed flowrate $F = 0.48$ kg/h and $S/F = 6$).
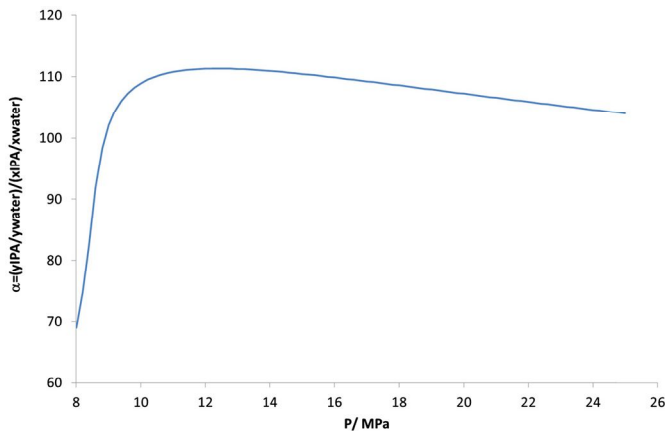

Fig. 8. Influence of pressure on selectivity of CO_2 at 40 °C, for a mixture composition representative of global mixture of the column ($z_{CO2} = 0.857$; $z_{IPA} = 0.007$; $z_{water} = 0.136$). Calculation done with the SRK-PSRK-UNIQUAC model.

IPA, whereas two theoretical stages slightly overestimate it, as shown in Fig. 9.

These results establish that, under these conditions, the value of the HETS lies between 1 and 2 m. Although this estimation is not accurate, the order of magnitude remains however quite high when comparing to the literature values, for the system CO_2/IPA/water, comprised between 0.1 and 0.4 m [12,13]. However, these literature values were issued from experimental data obtained on systems where supercritical CO_2 is the dispersed phase. Indeed, Bernad

et al. [14] have observed, for the CO_2/ethanol/water system, that this mode of operation lead to better separation performances than trickle bed operation. HETS values of a packed column ranged between 0.8 and 1.5 m in the trickle bed configuration, although it was reduced to 0.54–0.85 m in the bubble column mode.

So, our experimental results confirm the quite poor separation performances of the experimental set-up under trickle bed operating conditions. The low mass transfer performances could be due to poor wetting of the packing by the liquid phase, leading to low interfacial area. Indeed in very small diameter columns, it is suspected that a substantial portion of the liquid film flows preferentially along the inner walls of the contactor, leading to poor wetting of the packing.

4.2. Influence of solvent to feed ratio

The influence of the solvent to feed ratio (S/F) has been studied for operation at 10 MPa and 40 °C with a 5% (w/w) IPA feed and spring-shaped packing. The values of S/F ratios were chosen according to the technical limits of the pumps but also in order to avoid flooding of the column (detectable by the presence of a large amount of water in the separators, from entrainment of the liquid at the head of the column). The theoretical and experimental results in terms of IPA mass fraction and IPA and water recovery ratios in the raffinate are presented in Fig. 10.

In respect to IPA extraction, improved separation is obtained when S/F ratio increases from 3.95 to 11. Recovery ratios of both compounds decrease at the bottom of the column when the S/F ratio increases. Consequently, at high S/F ratio (11.04, Run 10) the
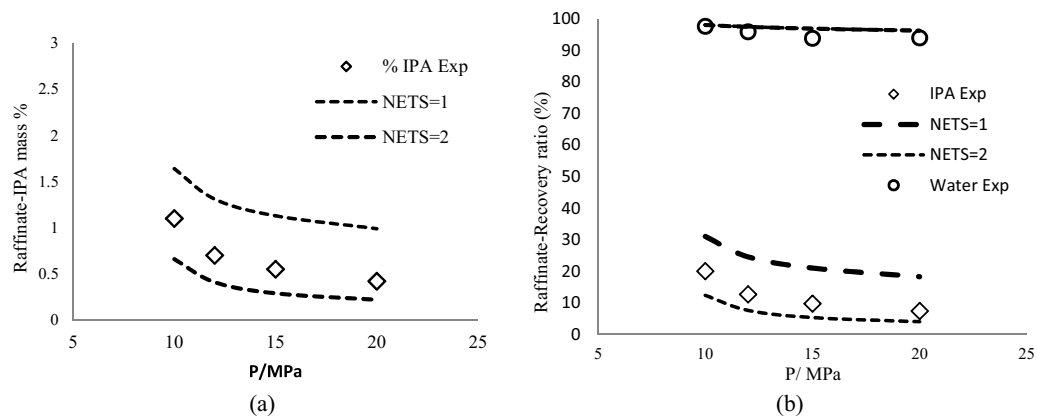

Fig. 9. Comparison of experimental and simulation results with NETS = 1 and 2 of (a) mass fraction of IPA in the raffinate and (b) recovery ratio of IPA and water in the raffinate (40 °C, feed flowrate $F = 0.48$ kg/h and $S/F = 6$).
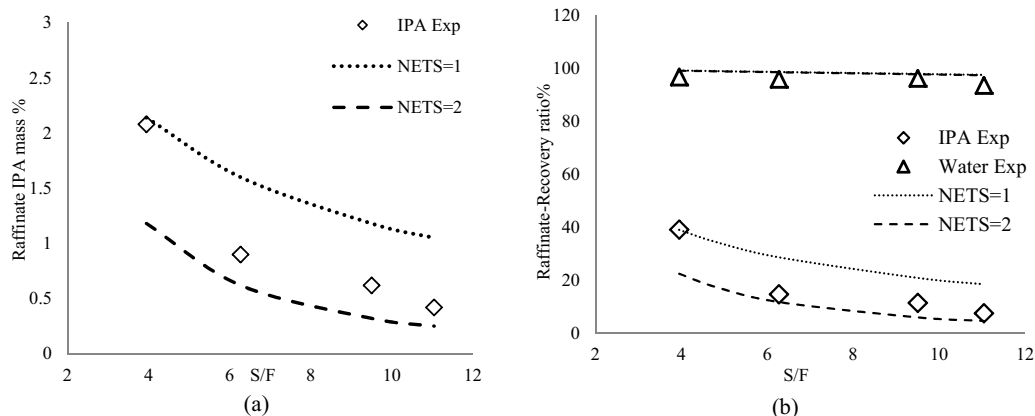
Fig. 10. Influence of S/F on the mass fraction of IPA and recovery ratios of water and IPA in the raffinate ($P = 10$ MPa, $T = 40\,°C$, $F = 0.48$ kg/h, 5% (w/w) IPA, spring packing).

recovery ratio of IPA in the extract phase obtained by mass balance is high (92.51%) but because of co-extraction of water, the corresponding purity is low (42.7%) and operation at high S/F ratio is therefore not advisable with the objective of obtaining pure IPA at the top of the column.

4.3. Influence of temperature

Influence of temperature was tested at 10 MPa in the range 40–60 °C (compatible with technical limitations of the set-up) in the case of a S/F ratio equal to 9.5. Experimental as well as calculated results are presented in Fig. 11 where calculation was performed in a broader range of temperature (from 40 to 90 °C). As could be expected from the decrease of the solvent power of CO_2 when temperature increases, it is observed that between 40 and 60 °C, recovery ratio of IPA in the raffinate phase is increasing with temperature. In this range of temperature, at 10 MPa, the diminishing solvent power of CO_2 leads to a decrease of solubility of water and IPA in the CO_2 phase. This phenomenon can be observed on IPA partition coefficient behaviour with temperature and pressure shown in Fig. 6. However, from calculated results, it can be noticed that this tendency reverses beyond 60 °C, due to the higher tendency of solute to vaporize. However temperature has to be increased over 90 °C to obtain a similar performance as for 40 °C. This has also been confirmed when evaluating the mutual solubility of the binary system IPA–CO_2. Solubility decreases when temperature increases up to 60 °C and then it increases over this temperature. This result demonstrates that at 10 MPa, 40 °C is a more favourable temperature to maximize recovery of isopropanol from water.

However, it has been shown in the previous section that, at 40 °C, the maximum theoretical IPA purity is 97% (w/w), while this limit disappears at 70 °C. Operating temperature has thus to be optimized according to the objective of separation, purity or recovery.

4.4. Influence of IPA composition of the feed

The composition of IPA in the feed was varied in the range 5–60% (w/w), at 10 MPa and 40 °C and at a solvent to feed ratio equal to 9.5. Fig. 12 shows experimental and simulation results.

When the IPA percentage in the feed increases, it is observed from experimental values that the composition of the raffinate remains almost constant and that IPA and water recovery ratios in the raffinate are decreasing. For a 60% (w/w) IPA feed (Run 5), experimental purity of water at the raffinate is found to be equal to 99.38% (w/w) leading with mass balance to a 99.69% IPA recovery ratio at the extract with a high purity (89.7%, w/w).

In this case of high IPA content in the feed, simulation yields better representation of experimental behaviour when the column is represented with three theoretical stages, meaning that HETS is decreased to 0.7 m. These results indicate better mass transfer, probably because change of physico-chemical properties of the liquid phase which contains much more IPA. In particular, Chun and Wilkinson [35] reported that the interfacial tension of the mixture CO_2–IPA–water decreases with increasing IPA mole fraction, in the same trend as density and viscosity. This evolution is likely to favourably modify the wetting properties of the liquid phase, resulting in better mass transfer. Similar trend was observed by Brunner and Budich [36] in the case of separation of ethanol–water mixtures at 333 K and 10 MPa in a packed column with reflux. HETS values where in the order of magnitude of 2 m for stripping and enriching sections in the case of low concentrated ethanol solutions and theses values dropped down to 0.5–1 m for solutions containing more than 60% ethanol. In addition to modification of these properties, the authors also mentioned that the thermodynamic model was less accurate at high ethanol content, which could yield erroneous too low values of HETS.

4.5. Influence of the column packing

As stated from our results, the separation efficiency of our column is low when comparing order of magnitude of fitted HETS (above 1 m) to values classically found in the literature and a possible explanation from the poor hydrodynamic conditions inside the column has been proposed. This phenomenon is indeed strongly suspected when considering the low value of the ratio "column diameter-characteristic length of the packing", ($\phi_{column}/\phi_{packing} \approx 4$), which could be responsible of non-negligible wall effects inside the column leading to wall channelling for the liquid. This hypothesis is moreover strengthened by the better results obtained for higher IPA content in the feed as stated in the previous section.

In an attempt to enhance mass transfer efficiency by improvement of flow conditions inside the column, random stainless steel spring packing was replaced by metallic foam packing described in Table 1. This type of structured packing has been shown to be very attractive in the case of countercurrent gas–liquid mass transfer operation, because of its high void fraction (92%), high liquid hold-up and low pressure drop [37]. With this packing, whose dimensions of elementary cylindrical elements have been carefully adjusted to internal column diameter, wall channelling is thus expected to be significantly reduced. However, note that its specific surface is lower than for spring-shaped packing. In Fig. 13, IPA and water recovery ratios in the raffinate are plotted as a function of
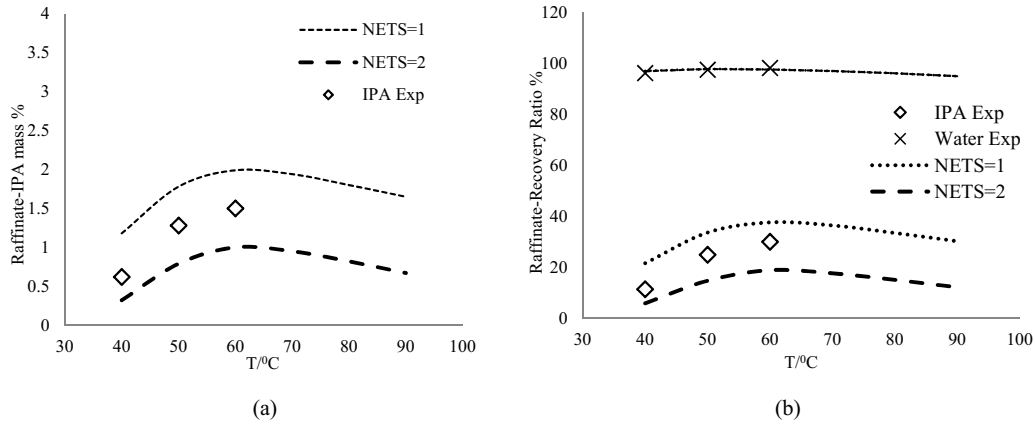
Fig. 11. Influence of the temperature on the mass fraction of IPA and recovery ratios of water and IPA in the raffinate (P = 10 MPa, F = 0.48 kg/h, S/F = 9.5, 5% (w/w) IPA, spring packing).

pressure, temperature and S/F ratio in the case of separation of a 5% (w/w) IPA feed. Experimental results are compared with results obtained with spring-shaped packing.

The first obvious conclusion from Fig. 13 is the low influence of the packing type on IPA and water recovery ratios. On a global point of view, IPA extraction is barely improved (lower IPA recovery ratios in the raffinate) in most experimental conditions, except at low solvent-to-feed ratio. Moreover, with the metallic foam packing, flooding of the column was observed at high pressure (20 MPa), where density difference between both phases is reduced. Also, another surprising result is the very low impact of operating temperature in the case of foam packing where recovery ratios appear almost constant in respect to temperature. Remember that, in the case of the spring shaped packing, temperature was shown to have a negative effect and this was correctly explained by thermodynamic considerations. Here a possible explanation may arise from a low heat transfer efficiency of the foam packing. Indeed, liquid feed is only preheated to 40 °C and packing serves also as a heat exchanger for the liquid to reach 60 °C. Although the metallic foam cylinders are adjusted to the internal column diameter, it is very likely that there are only very few contact points between the packing and the wall, much less than with the spring-shaped packing. Associated with the poorer thermal conductivity of the foam material (FeCrAlY conductivity is 16 W m^{-1} K^{-1} compared to 26 W m^{-1} K^{-1} for stainless steel) and with the higher porosity of the foam, this leads to low effective thermal conductivity and to low heat transfer from wall towards the liquid flow. So it can be imagined than the liquid flow is not correctly heated to up to 60 °C when flowing along the column equipped with the foam packing. Actually, the separation was probably not

performed at 60 °C in the whole column in the case of the foam packing.

The low influence of packing type on mass transfer seems to contradict our previous hypothesis about liquid wall channelling and this could mean that flowing of liquid phase is actually not of film type on the packing, but rather as falling droplets. In this case, packing would only have a slight influence as a steric hindrance for freely falling droplets. So, further specific experiments would be needed to visualize flowing of liquid on the packing and investigate the flow characteristics inside the column. Non-intrusive tomographic techniques have been tested in the literature to investigate the fluid distribution in packed columns [38]. As an interesting example, X-ray tomography is a mature technique which combines high spatial resolution, material compatibility and flexibility required to investigate, both qualitatively and quantitatively, the axial and radial distribution of multiphase flows in lab scale packed columns. The literature studies using this technique are promising and show that liquid distribution in the packing but also characteristics of the packing, such as liquid hold-up [39], or interfacial area [40], can be evaluated. Use of such techniques could bring useful fundamental knowledge about liquid–fluid flows in high pressure separation columns and thus help understanding mass transfer performances.

4.6. Use of simulation to propose strategies to improve the separation

Process simulation has been done to assess the influence of the number of theoretical stages on the necessary S/F ratio in the case of a 5% (w/w) IPA feed and for a given target of 90% IPA recovery in the extract. This latter specification was imposed on the outgoing
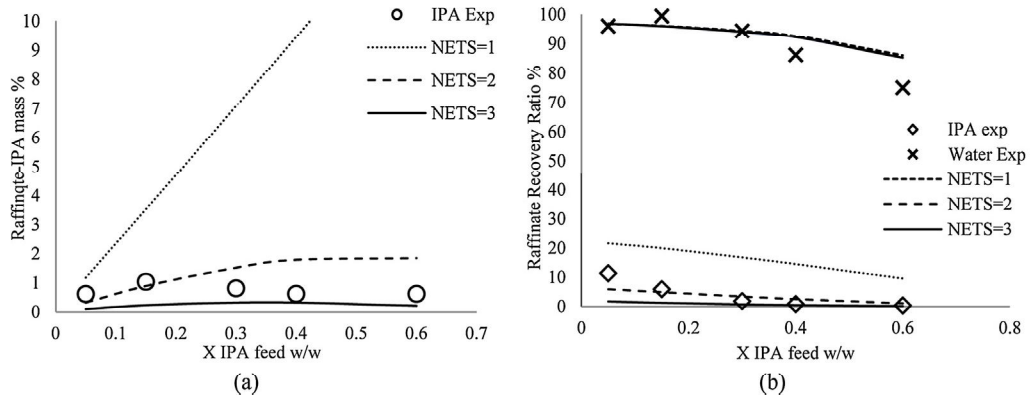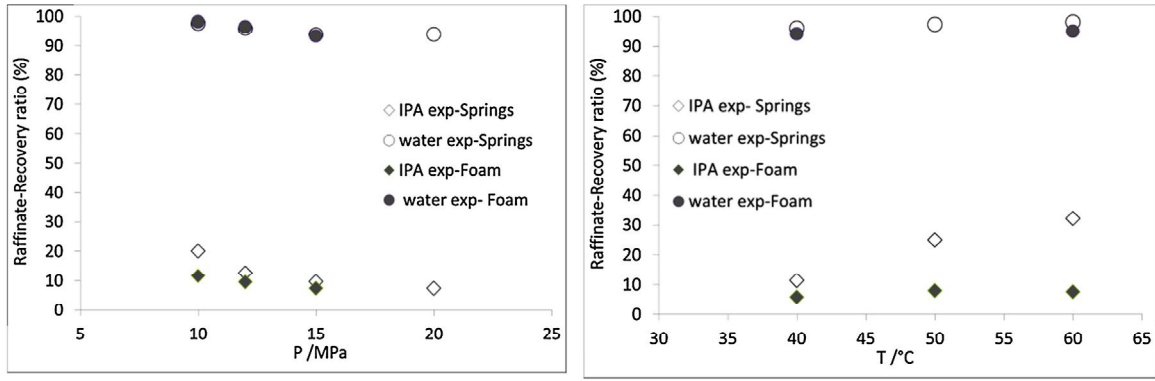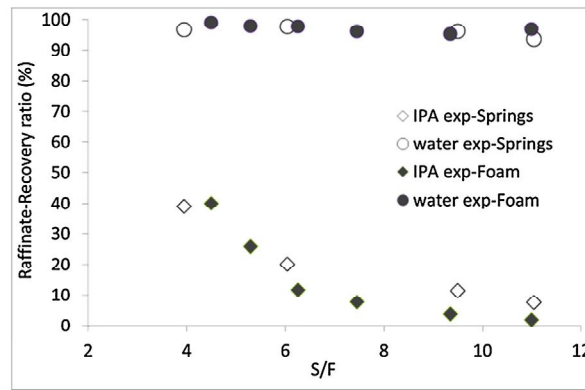

Fig. 12. Influence of feed IPA content on the mass fraction of IPA (a) and recovery ratios (b) in the raffinate (10 MPa, 40 °C, F = 0.48 kg/h, S/F = 9.5, spring packing).

(a) T=40°C-S/F=6

(b) P=10 MPa-S/F=9.5

(c) T=40°C-P=10 MPa

Fig. 13. Influence of type of packing of the column on raffinate recovery ratios. 5% (w/w) IPA content in the feed at different pressures (a), different temperatures (b) and solvent to feed ratio (c).

stream at the top of column by acting on the CO_2 flowrate (*i.e.*, on the *S/F* ratio), and results are shown in Fig. 14. It is observed that in this case a maximum 83% IPA mass fraction in the extract can be obtained with a 90% IPA recovery at the top, and that 12 theoretical stages are needed to reach this target. This result is not surprising as it was mentioned that, for a type I phase diagram, there is a theoretical limit for the purity, irrespectively of the efficiency of mass transfer. The next option would be to choose operating conditions for type II diagram, for example 70 °C and 10 MPa, as shown in Fig. 4. Nevertheless, from simulation results presented in Fig. 14 it is seen that at 70 °C high IPA mass fraction

in the extract are not obtained in our standard configuration of the column, even using a high number of theoretical stages. To overcome this limit, implementation of a reflux (internally or externally generated) at the top of the column, would be necessary, as proposed by Brunner [11] for ethanol separation. In this case, there is no theoretical limit for the purity of the extract. Note that type II diagram of Fig. 4 exhibits a very narrow right side of the biphasic curve that implies very accurate calculations that are out of the scope of this work. Such work was proposed for instance by Maschietti and Pedacchia [41], who compared, thanks to simulation, internal and external reflux configurations in the case of fish oil esters fractionation.

5. Conclusion

This study has confirmed the feasibility of the continuous operation of purification of an aqueous phase containing isopropanol, using supercritical CO_2 as the separation agent. Influence of operating conditions on the separation performances were investigated on the range of experimental conditions compatible with our experimental set-up. The thermodynamic behaviour of the CO_2–IPA–water system under pressure was satisfactorily represented for the whole range of conditions corresponding to the process, using the predictive Soave Redlich Kwong model (SRK) modified by Boston Mathias with PSRK mixing rules and using the UNIQUAC model for activity coefficients calculations. The experimental results were then compared to simulation, and order of magnitude and trends for HETS values were calculated by fitting experimental results with calculations done using the Prosim Plus
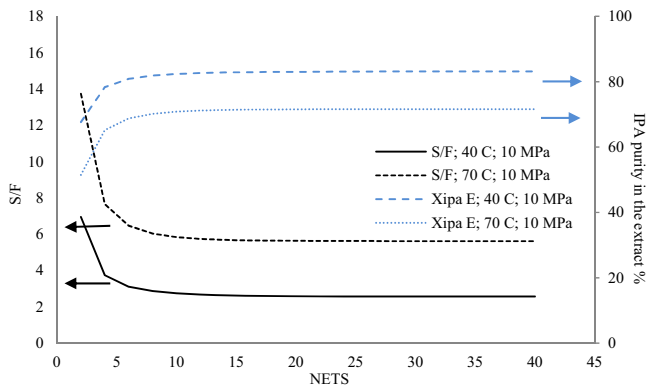

Fig. 14. Influence of the NETS on the *S/F* ratio and the consequent extract IPA purity in the case of a 5% (w/w) IPA feed and a target of 90% IPA recovery ratio in the extract.

software. HETS values were found to be above 1 m, when the feed contained 5% (w/w) of IPA and were shown to diminish when this composition was increased to 60% (w/w).

The set-up allowed reaching good IPA recovery at the top of the column, but IPA could not be obtained with high purity. Experimental conditions for better IPA purification are thus to be found in order to propose conditions of recovery of high purity bio-isopropanol. On an experimental point of view, improvement of the hydrodynamics in the existing column in order to improve mass transfer and decrease the HETS seems to be necessary. For this purpose, better control of the liquid flow inside the column would be required, and visualization of inner flows in general would be helpful. This means designing a specific experimental device dedicated to visual observation. Moreover, designing a contactor with a reflux section, could lead to the determination of operating conditions allowing extract enrichment.

Nevertheless, although convenient, the NETS/HETS approach is somewhat limited for that purpose, giving the low generalization capability of this concept. Indeed, the experimental NETS is expected to vary when a reflux is operated in the column, so that it might be not suitable to use NETS calculated in this study to predict what would happen when operating the column with internal (with gradient temperature) or external reflux. A more reliable approach should be thus to model the multicomponent mass transfer inside the contactor thanks to the so-called "rate-based" or "non-equilibrium" approach, taking into account mass-transfer kinetics between phases, as proposed by Martin and Cocero [42]. This kind of modelling is available in commercial simulation softwares such as Aspen Plus or ProSim Plus. Its use in the context of supercritical fractionation of aqueous mixtures of isopropanol is promising and its potentiality is now under investigation in our group.

References

[1] O.E. Logsdon, A.L. Richard, Isopropyl alcohol, in: Kirk-Othmer Encyclopedia of Chemical Technology, John Wiley & Sons, 2000.
[2] M. Matsumura, S. Takehara, H. Kataoka, Continuous butanol/isopropanol fermentation in down-flow column reactor coupled with pervaporation using supported liquid membrane, Biotechnology and Bioengineering 39 (1992) 148–156.
[3] K. Inokuma, J.C. Liao, M. Okamoto, T. Hanai, Improvement of isopropanol production by metabolically engineered *Escherichia coli* using gas stripping, J, Bioscience and Bioengineering 110 (2010) 696–701.
[4] I. Medina, J.L. Martinez, Dealcoholisation of cider by supercritical extraction with carbon dioxide, J. Chemical Technology and Biotechnology 68 (1997) 14–18.
[5] C. Da Porto, D. Decorti, Countercurrent supercritical fluid extraction of grape-spirit, J. Supercritical Fluids 55 (2010) 128–131.
[6] C. Schacht, C. Zetzl, G. Brunner, From plant materials to ethanol by means of supercritical fluid technology, J. Supercritical Fluids 46 (2008) 299–321.
[7] L. Vázquez, A.M. Hurtado-Benavides, G. Reglero, T. Fornari, E. Ibáñez, F.J. Señoráns, Deacidification of olive oil by countercurrent supercritical carbon dioxide extraction: experimental and thermodynamic modelling, J. Food Engineering 90 (2009) 463–470.
[8] V. Riha, G. Brunner, Separation of fish oil ethyl esters with supercritical carbon dioxide, J. Supercritical Fluids 17 (2000) 55–64.
[9] M. Budich, S. Heilig, T. Wesse, V. Leibküchler, G. Brunner, Countercurrent deterpenation of citrus oils with supercritical CO_2, J. Supercritical Fluids 14 (1999) 105–114.
[10] R. Valsecchi, F. Mutta, U. De Patto, C. Tonelli, Countercurrent fractionation of methylol-terminated perfluoropolyoxyalkylene oligomers by supercritical carbon dioxide, J. Supercritical Fluids 88 (2014) 85–91.
[11] G. Brunner, Counter-current separations, J. Supercritical Fluids 47 (2009) 574–582.
[12] P.J. Rathkamp, J.L. Bravo, J.R. Fair, Evaluation of packed columns in supercritical extraction processes, Solvent Extraction and Ion Exchange 5 (1987) 367–391.
[13] R.J. Lahiere, J.R. Fair, Mass-transfer efficiencies of column contactors in supercritical extraction service, Industrial and Engineering Chemical Research 26 (1987) 2086–2092.
[14] L. Bernad, A. Keller, D. Barth, M. Perrut, Separation of ethanol from aqueous solutions by supercritical carbon dioxide – comparison between simulations and experiments, J. Supercritical Fluids 6 (1993) 9–14.
[15] J.S. Lim, Y.-W. Lee, J.-D. Kim, Y.Y. Lee, H.-S. Chun, Mass-transfer and hydraulic characteristics in spray and packed extraction columns for supercritical carbon dioxide–ethanol–water system, J. Supercritical Fluids 8 (1995) 127–137.
[16] G. Budich, G. Brunner, Supercritical fluid extraction of ethanol from aqueous solutions, J. Supercritical Fluids 25 (2003) 45–55.
[17] A. Laitinen, J. Kaunisto, Supercritical fluid extraction of 1-butanol from aqueous solutions, J. Supercritical Fluids 15 (1999) 245–252.
[18] G. Brunner, Industrial process development: countercurrent multistage gas extraction (SFE) processes, J. Supercritical Fluids 13 (1998) 283–301.
[19] V. Riha, G. Brunner, Separation of fish oil ethyl esters with supercritical carbon dioxide, J. Supercritical Fluids 17 (2000) 55–64.
[20] L. Fiori, M. Manfrini, D. Castello, Supercritical CO_2 fractionation of omega-3 lipids from fish by-products: plant and process design, modeling, economic feasibility, Food and Bioproducts Processing 92 (2014) 120–132.
[21] E.B. Moraes, C.J.G. Vasconselos, M.R. Wolf Maciel, Simulation and optimization of the supercritical extraction process applied to complex mixtures, in: Proceedings of the 6th World Congress of Chemical Engineering, Melbourne, 2001.
[22] S. Camy, J.-S. Condoret, Modelling and experimental study of separators for co-solvent recovery in supercritical extraction process, J. Supercritical Fluids 38 (2006) 51–61.
[23] A.P. Bünz, N. Zitko-Stemberger, R. Dohrn, Phase equilibria of ternary and quaternary systems containing carbon dioxide, water, isopropanol, and glucose, J. Supercritical Fluids 7 (1994) 43–50.
[24] B.S. Chun, G.T. Wilkinson, Ternary phase equilibria of the iso-propanol + water + carbon dioxide system at high pressure, Korean J. Chemical Engineering 16 (1999) 187–192.
[25] M.J. Huron, J. Vidal, New mixing rules in simple equations of state for representing vapour–liquid equilibria of strongly non-ideal mixtures, Fluid Phase Equilibria 3 (1979) 225–271.
[26] G. Soave, Equilibrium constants from a modified Redlich–Kwong equation of state, Chemical Engineering Science 27 (1972) 1197–1203.
[27] J.F. Boston, P.M. Mathias, Phase equilibria in a third-generation process simulator, in: Proceedings of the 2nd International Conference on Phase Equilibria and Fluid Properties in the Chemical Process Industries, West Berlin, 1980, pp. 823–849.
[28] T. Holderbaum, J. Gmehling, PSRK: a group contribution equation of state based on UNIFAC, Fluid Phase Equilibria 70 (1991) 251–265.
[29] D.S. Abrams, J.M. Prausnitz, Statistical thermodynamics of liquid mixture: a new expression for the excess Gibbs energy of partly or complete miscible systems, AIChE J. 21 (1975) 116–128.
[30] T.F. Anderson, J.M. Prausnitz, Application of the UNIQUAC equation to calculation of multi-component phase equilibria: 1. Vapor–liquid equilibria, Industrial Engineering Chemical Process Design Development 17 (1978) 552–560.
[31] M. Radosz, Vapor–liquid equilibrium for 2-propanol and carbon dioxide, J. Chemical Engineering Data 31 (1986) 43–45.
[32] R. Wiebe, V.L. Gaddy, The solubility in water of carbon dioxide at 50, 75 and l00 °C, at pressures to 700 atmospheres, J. American Chemical Society 61 (1939) 315–318.
[33] G. Houghton, A.M. McLean, P.D. Ritchie, Compressibility, fugacity, and water-solubility of carbon dioxide in the region 0–36 atm and 0–100 °C, Chemical Engineering Science 6 (1957) 183–187.
[34] F. Barr-David, B.F. Dodge, Vapor–liquid equilibrium at high-pressures. The systems ethanol–water and 2-propanol–water, J. Chemical Engineering Data 4 (1959) 2214–2219.
[35] B.-Y. Chun, G.T. Wilkinson, Interfacial tension in high-pressure carbon dioxide mixtures, Industrial Engineering Chemistry Research 34 (1995) 4371–4377.
[36] G. Brunner, M. Budich, Separations of organic compounds from aqueous solutions by means of supercritical carbon dioxide, in: G. Brunner (Ed.), Supercritical Fluids as Solvents and Reaction Media, Elsevier, Amsterdam, 2004, pp. 489–522.
[37] J. Levêque, D. Rouzineau, M. Prevost, M. Meyer, Hydrodynamic and mass transfer efficiency of ceramic foam packing applied to distillation, Chemical Engineering Science 64 (2009) 2607.
[38] C.E. Schmit, D. Cartmel, R.B. Eldridge, Process tomography: an option for the enhancement of packed vapor–liquid contactor model development, Industrial Engineering Chemistry Research 39 (2000) 1546–1553.
[39] A. Viva, S. Aferka, D. Toye, P. Marchot, M. Crine, E. Brunazzi, Determination of liquid hold-up and flow distribution inside modular catalytic structured packings, Chemical Engineering Research and Design 89 (2011) 1414–1427.
[40] S. Aferka, P. Marchot, M. Crine, D. Toye, Interfacial area measurement in a catalytic distillation packing using energy X-ray CT, Chemical Engineering Science 65 (2010) 511–516.
[41] M. Maschietti, A. Pedacchia, Supercritical carbon dioxide separation of fish oil ethyl esters by means of a continuous countercurrent process with an internal reflux, J. Supercritical Fluids 86 (2014) 76–84.
[42] A. Martin, M.J. Cocero, Mathematical modelling of the fractionation of liquids with supercritical CO_2 in a countercurrent packed column, J. Supercritical Fluids 39 (2007) 304–314.